Dynamics of polymer electrolyte with LiTFSI via Quasi-Elastic Neutron Scattering

Hui Wang[1], *Naresh C.* Osti[2], *Jürgen* Allgaier[1], *Marcella Cabrera* Berg[3], *Rene* Halver[1], *Eugene* Mamontov[2], *Godehard* Sutmann[1, 4], *Yuya* Doi[5], *Nicolas* Bucher[6], *Takeshi* Egami[7], *Stephan* Förster[1], and *Michael* Ohl[1, 7]

[1]Research Center Jülich, 52428 Jülich, Germany
[2]Neutron Scattering Division, Oak Ridge National Laboratory, Oak Ridge, TN 37831, USA
[3]Department of Physics, University of Regina, Saskatchewan S4S 0A2, Canada
[4]Interdisciplinary Center for Advanced Materials Simulations (ICAMS), Ruhr-University Bochum, 44801 Bochum, Germany
[5]Department of Materials Physics, Nagoya University, Nagoya, Aichi 4648603, Japan
[6]Varta Microbattery GmbH, 73479 Ellwangen, Germany
[7]Department of Materials Science and Engineering, Univ. Tennessee, Knoxville TN. 37996, USA

Abstract. Most lithium batteries offer a wide range of applications. However, safety issues are still an unresolved issue for several applications. To solve the safety issue of Li-ion batteries, solid polymer electrolyte is a promising candidate to replace commercial liquid electrolyte. A 4-arm star poly(ethylene oxide) polymer with LiTFSI salt as an electrolyte was studied. The dynamics of this polymer were explored with the Quasi-Elastic Neutron Scattering technique. Furthermore, the influence of temperature and Li salt concentration on the polymer dynamics was investigated. The dynamics of the polymer ends of the arm show much higher flexibility than the core parts making those types of polymers attractive for further studies in battery research.

Li-ion batteries (LIBs) play a key role in our everyday lives as a component of electronic devices such as mobile phones and electric vehicles [1, 2]. They are also employed as high-density energy storage source in various industries, such as power plants, military equipment, and aerospace. In spite of their wide use, LIBs suffer from some shortcomings, such as the low boiling point of the commercial liquid electrolyte, which poses safety risks, including leaks, burning, and explosions [3, 4]. Solid polymer electrolytes (SPEs) stand out as promising potential replacements due to their high energy density, lightweight, and flexibility and attract a lot of research interests [5, 6]. These batteries could greatly improve the way we power our devices [7]. However, the ionic conductivity of SPEs is still not ideal, which is one of the significant obstacles to their wide application [8]. An assumption was proposed that the polymer segmental, backbone motions, and Li-ion charge transport are closely correlated [5]. Do et al. observed a strong coupling between conductivity and the relaxation of the polymer electrolyte [9], verifying the assumption experimentally. They found that cages are formed with about 5-6 EO monomer units surrounding the Li–ion and the cage decay time is about 5 ns. They assumed that the flexibility of the PEO chain reduces the cage decay time resulting in an increase in Li–ion transport. In this paper, the dynamics of the 4-arm star poly(ethylene oxide) (4armPEO) and the effect of LiTFSI will be investigated with Quasi-Elastic Neutron Scattering (QENS).

The 4armPEO (M_w=13.8 kg/mol, *PDI*=1.01), as illustrated in Fig. 1, was synthesized by polymerizing ethylene oxide (EO) (Sigma-Aldrich, ≥ 99.9%) and ethylene oxide-d4 (Cambridge Isotope Laboratories, 98% D) with partially potassium metalated pentaerythritol as initiator in anhydrous DMSO in our deuteration laboratory [10]. With the experience of our previous studies [11], we surmise that Li+ is attracted by the ether-O of the core part and tends to be trapped in the area close to the center carbon atom. To study the dynamics of the core and the hand parts of the polymer (as shown in Fig. 1 (a)) separately, the partially deuterated samples were also synthesized. The arm lengths are about 72 EO monomer units and, when fully stretched, are about 200 Å long. For the deuteration, either the first 36 EO units close to the core (core-deuterated 4armPEO, M_w=12.8 kg/mol, *PDI* = 1.05) or the last 36 EO units close to the end (hand-deuterated 4armPEO, M_w=13.9 kg/mol, *PDI* = 1.07) were selected. Additionally, Lithium bis(trifluoromethanesulfonyl)imide (LiTFSI) was added to the 4armPEO as the source of Li+. QENS was conducted on original and deuterated 4armPEO samples with varying amounts of LiTFSI (as listed in Table 1) using a backscattering silicon spectrometer (BASIS) of the Spallation Neutron Source at Oak Ridge National Laboratory, USA [12]. Samples were sealed in a flat plate Aluminum sample holder and measured under He environment. The energy of the Neutron beam is 2.08 μeV (λ=6.4 Å). The sample was heated to 400 K, equilibrated for 10 minutes, and then cooled to 380 K, 360 K, 340 K, 300 K, 280 K, and 260 K for measurement (Fig. 1(b)). The instrument was set up to get a reflection from Si(111) analyzers panel covering the Q range of 0.3 $Å^{-1}$ to 1.9 $Å^{-1}$and the energy transfer window of -120μeV to 120 μeV with an instrumental energy resolution of 3.5 μeV. The

resolution was measured separately from each sample at 20 K.

Table 1. Sample List

Sample Name	Deuterated part of 4armPEO	Proportion of LiTFSI
4armPEO	No	0
4armPEO + 20% LiTFSI	No	20 w.t.%
4armPEO + 40% LiTFSI	No	40 w.t.%
Core Deuterated 4armPEO	Core part	0
3Core Deuterated 4armPEO + 20% LiTFSI	Core part	20 w.t.%
Hand Deuterated 4armPEO	Hand part	0
Hand Deuterated 4armPEO + 20% LiTFSI	Hand part	20 w.t.%

The QENS spectra of 4armPEO with 0%, 20%, and 40% LiTFSI are shown in Fig. 2 (a), (b), and (c). The QENS spectra below 320 K are sharp and intense, whereas peaks collected above 320 K exhibits considerable broadening. There is a discontinuity at 340 K of 4armPEO with 0% and 20% LiTFSI, but not in 4armPEO with 40% LiTFSI. Meanwhile, DSC measurements reveal melting peaks at around 320 K for 4armPEO with 0% and 20% LiTFSI, while there is no prominent peak for 4armPEO with 40% LiTFSI (Fig. 3). It became evident that with the increase of the Li – salt content, the melting peak is suppressed, making the system softer. In addition, higher Li–salt content makes a better battery system that can function at lower temperatures. Because of the higher scattering cross section, H atoms from 4armPEO contribute most of the Neutron scattering signal. Therefore, the QENS data and the DSC results suggest a significant change in the dynamics of the polymer after melting in the samples with 0% and 20% LiTFSI content.

The QENS spectrum comprises of the elastic–incoherent structure factor (EISF) and the quasi-elastic scattering. The spectra were fitted using delta and Lorentzian functions convoluted with the instrument resolution measured from the same sample at 20K (Fig. 4). Below the melting temperature, the QENS spectra could be fitted using a single Lorentzian, which can be assigned to a localized motion of Hydrogen atoms in 4armPEO (Model I, Equation 1). Above the melting temperature, two Lorentzians, one for fast and another for slow dynamics (Mode II, Equation 2), were needed. Among them, the narrower component captures the slower diffusion process of 4armPEO.

$$S(Q,\omega) = A(Q)\delta(\omega) + B(Q)L(Q,\omega) \quad \text{(Mode I)} \quad (1)$$

$$S(Q,\omega) = A(Q)\delta(\omega) + B(Q)L_{fast}(Q,\omega) + C(Q)L_{slow}(Q,\omega) \quad \text{(Mode II)} \quad (2)$$

The EISF and the half width at half maximum (HWHM) were obtained from the fitting of the QENS spectrum. The EISFs of 4armPEO below the melting temperature (320 K) do not show a strong decay suggesting a strong elastic neutron scattering over the length scales from appr. 3 Å to 20 Å. This is attributed to the relatively slow motion of the H atoms of 4armPEO below the melting temperature. However, the EISFs above the melting temperature drop to 0.2.This reduction in EISF indicates that more than 80% of the elastic scattering was

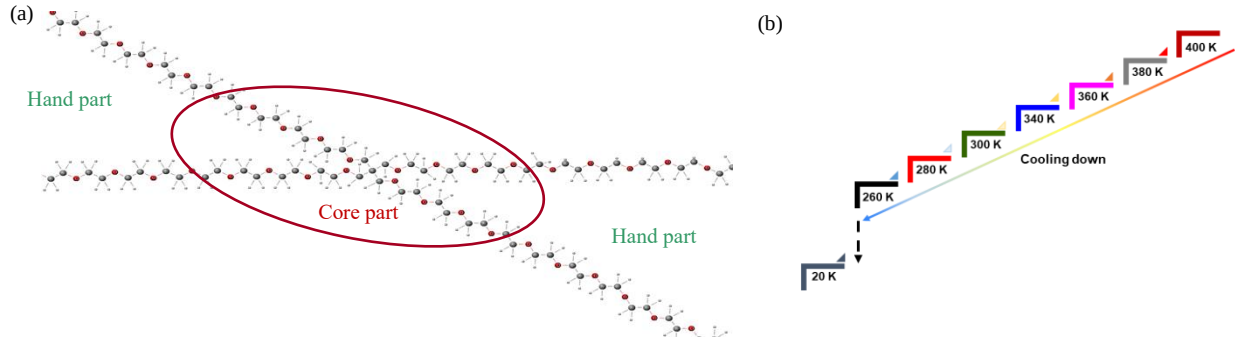

Figure 1. Snapshot of a Molecular structure of (a) 4armPEO, red balls represent oxygen atoms, the black balls represent carbon atoms, and the small white balls represent hydrogen atoms; (b) Temperature steps at which QENS data were collected during the cooling process. Note, in Fig.1a the core part and hand part consist just of about 3-5 monomer units for better illustration of the principal idea. In our samples the core part and hand parts when deuterated where about 36 monomer units each.

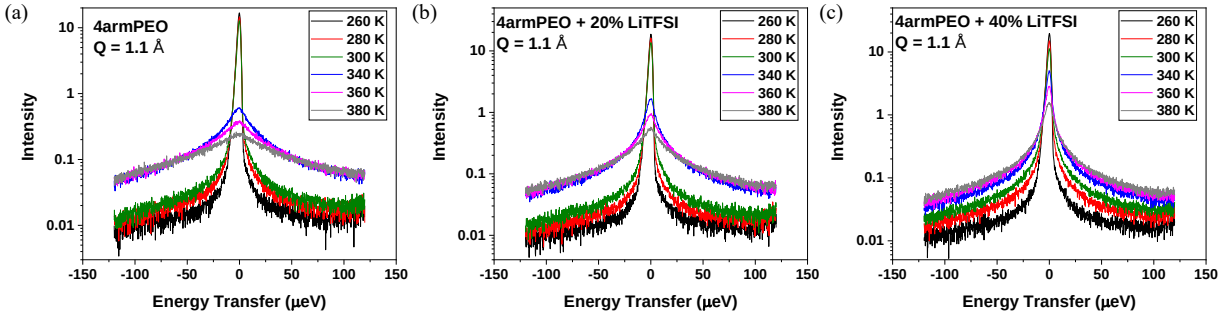

Figure 2. Representative QENS patterns for (a) 4armPEO, (b) 4armPEO+20%LiTFSI, and (c) 4armPEO+40%LiTFSI samples at a Q = 1.1 $Å^{-1}$.

transformed into inelastic scattering after the melting temperature. The H atoms move at a relatively low frequency below 320 K. Hence, the corresponding HWHMs from the Lorentzian were small, below 15 μeV, as shown in Fig. 5(b). While, QENS signals get broader after melting with HWHMs reaching 80 μeV (Fig. 5 (c)).

Assuming the plateau region in Fig. 5(b) is limited to a maximum Q = 1.25 Å^{-1} we can calculate the proper confinement radius r_{conf} according to the Volino-Dianoux confined diffusion model [13, 14] with $r_{conf} = \pi/Q = 2.5$ Å. This is in agreement to the literature and additional MD simulations we performed. It would lead to a spherical confinement volume of about 62 Å^3.

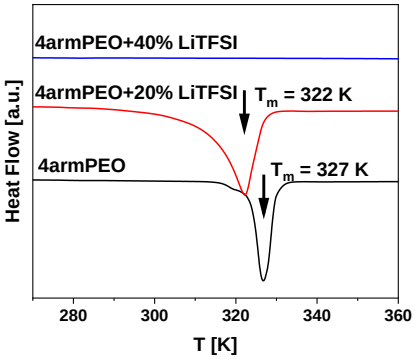

Figure 3. DSC profile for 4armPEO, 4armPEO+20%LiTFSI, and 4armPEO+40%LiTFSI samples.

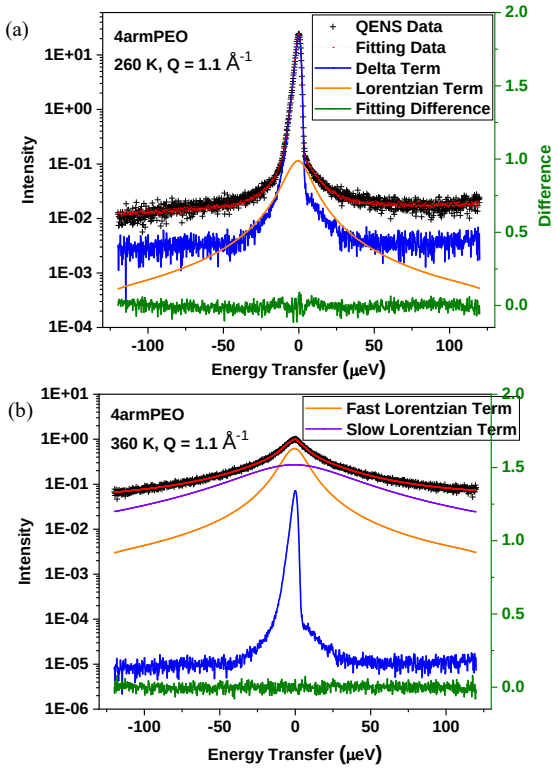

Figure 4. QENS spectra together with the model fit of 4armPEO at Q=1.1 Å^{-1} (a) from a single component fit below the melting temperature 320 K and (b) using two components fit above 320 K.

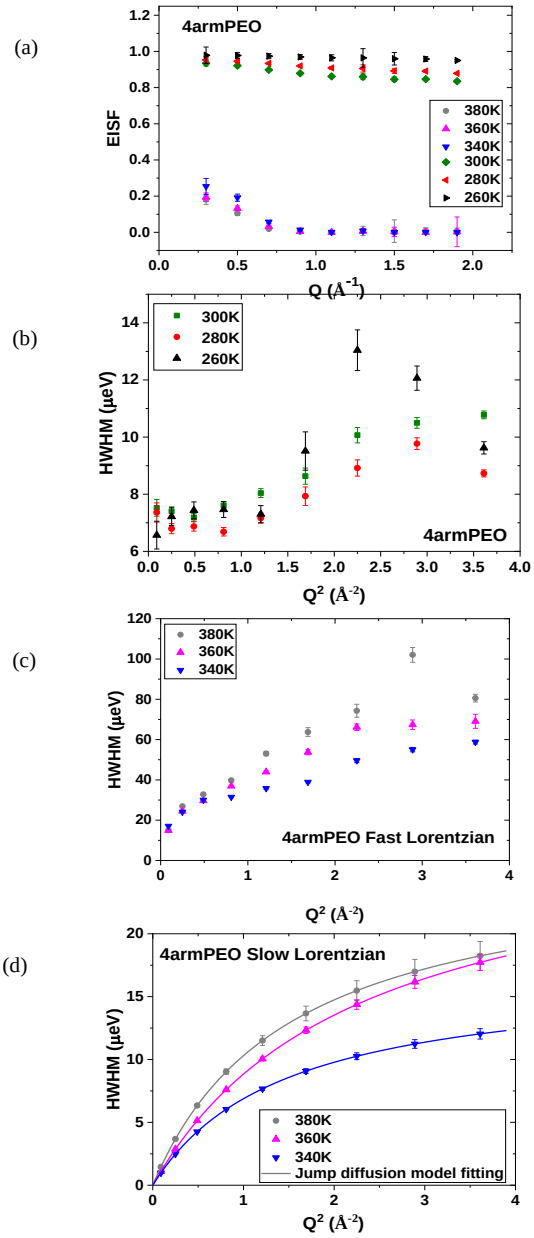

Figure 5. Q dependence of fitting parameters of 4armPEO. (a) EISF; (b) HWHM of the QENS spectra below 320 K; (c) and (d) are the HWHMs of the fast and slow components QENS spectra collected above 320K.

A comparison of the HWHMs of the broad component (Fig. 6) indicates that the adding LiTFSI slows down the chain dynamics. Furthermore, the narrower component (Fig. 5 (d)) observed after melting was fitted using the jump-diffusion model to obtain the diffusion coefficient, *D*, of this dynamics process (Equation 3).

$$\Gamma = \frac{DQ^2}{1+DQ^2\tau} \quad (3)$$

Table 2 shows that the diffusion coefficients of 4armPEO increase with temperature as expected. However, the addition of LiTFSI leads to a decrease in diffusivity values. Theoretically, the core-deuterated polymer should have a higher diffusivity than the hand-deuterated polymer, as the hand part of 4armPEO is more flexible than the core part. However, QENS results

show that the D values of the core-deuterated and hand-deuterated polymers are similar, likely due to the long arm of 4armPEO (with around 72 EO monomers on each arm), which smears out the effect of the constrained core part. It is unclear why the D values for the partially deuterated polymers are consistently smaller than that of 4armPEO. Still, it may be related to the larger molecular weight of the deuterated 4armPEO. Also, when adding Li salt, the diffusion coefficient decreases (Fig. 8). Here, Li – ions bind with the oxygen in the 4armPEO and reduce mobility. The addition of more of the Li – ions is found to restrict the mobility of the polymer chain further.

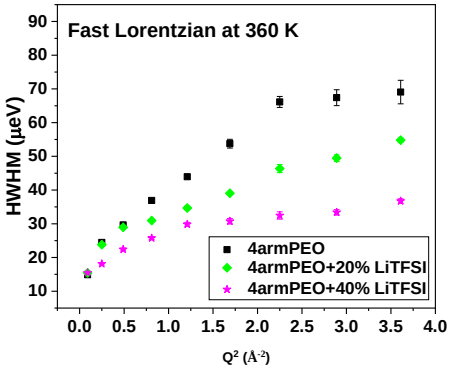

Figure 6. A comparison of HWHM of the fast Lorentzian component for 4armPEO, 4armPEO+20%LiTFSI, and 4armPEO+40%LiTFSI samples at 360 K.

Table 2. Diffusion coefficient of different samples at temperatures above T_m

Sample	D at 340 K (10^{-10} m^2/s)	D at 360 K (10^{-10} m^2/s)	D at 380 K (10^{-10} m^2/s)
4armPEO	1.76±0.03	1.93±0.03	2.59±0.05
4armPEO+20%LiTFSI	1.07±0.02	1.60±0.03	1.86±0.04
4armPEO+40%LiTFSI	1.02±0.03	0.88±0.02	1.17±0.02
Core Deuterated 4armPEO	1.43±0.03	1.71±0.04	1.90±0.02
Core Deuterated 4armPEO+20%LiTFSI	0.91±0.02	1.35±0.02	1.49±0.03
Hand Deuterated 4armPEO	1.25±0.02	1.53±0.03	1.70±0.04
Hand Deuterated 4armPEO+20%LiTFSI	0.93±0.02	1.23±0.02	1.45±0.02

With increasing temperature, the thermal activation triggers, not just for the polymer chain but also for the Li – ions, making them move faster and consequently raising the diffusion coefficient (Figures 7 and 8). In addition, the hands-deuterated 4armPEO has a smaller diffusion coefficient than the core deuterated at all temperatures and concentrations (Fig. 7). The core part moves slower than the hand part, which is what we expected to achieve.

The diffusion coefficients of the slow process follow the Arrhenius behavior. The activation energy,E_a, of this slow process is depicted in Fig. 7 and Fig. 8. The activation energy for the 4armPEO system is 10 mJ/mol, which agrees with the values in the literature [15]. Table 3 demonstrates that the activation energy increases with the addition of LiTFSI, indicating that the polymer chain motions get more restricted by the ions. Additionally, the activation energy for the core-deuterated and hand-deuterated samples is similar due to the long chains of the four arms in 4armPEO. The overall trend of the activation energy is consistent with that of the diffusion coefficients showing the restrictions of the chain dynamics with increasing Li – salt concentration due to the engagement of more of the Li-ions. Also, the hand part of the chain shows higher flexibility (diffusion coefficients), which is of great advantage for Li-ion transportation in batteries.

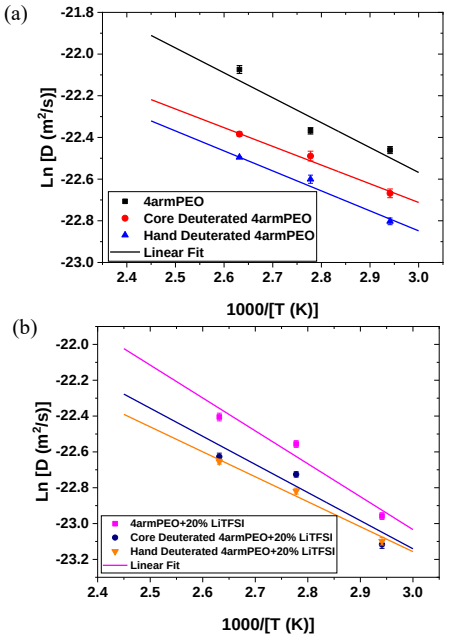

Figure 7. Temperature dependence of diffusivity showing an Arrhenius behavior.

Table 3. Activation energy of slow dynamics of different samples at temperatures above T_m

Sample	E_a (kJ/mol)
4armPEO	9.94±3.79
4armPEO+20%LiTFSI	15.27±3.55
4armPEO+40%LiTFSI	16.2
Core Deuterated 4armPEO	7.46±0.68
Core Deuterated 4armPEO+20%LiTFSI	13.05±5.05
Hand Deuterated 4armPEO	7.97±0.77
Hand Deuterated 4armPEO+20%LiTFSI	11.59±1.47

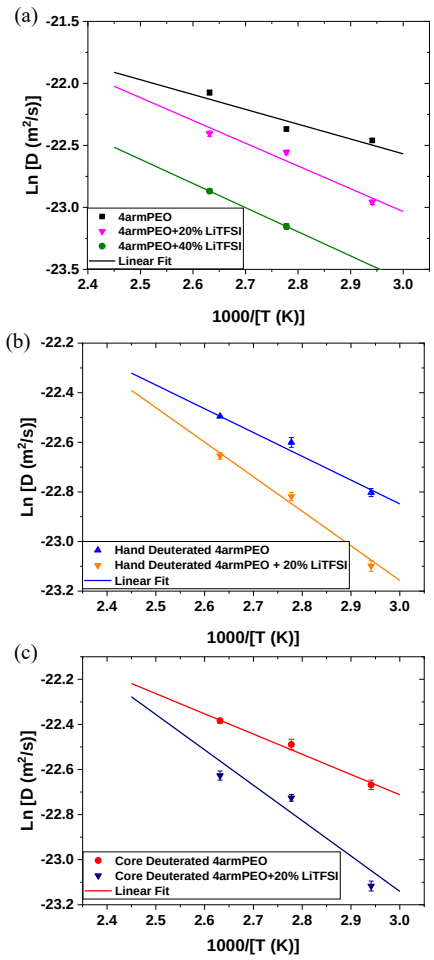

Figure 8. Temperature dependence of diffusivity showing an Arrhenius behavior.

To summarize, the present study investigates dynamics of 4armPEO and the influence of LiTFSI. Below the melting temperature, the H atoms move relatively slow resulting in the strong elastic neutron scattering. Above the melting temperature, two dynamics processes were observed: a faster-localized and a long-range slow process. The relative fast motions of H atoms cased the significant inelastic neutron scattering (EISF below 0.2). All dynamics processes observed here become faster with increasing temperature as expected. The addition of LiTFSI softens 4armPEO and contributes to its room temperature application. However, it also slows down the polymer dynamics by forming bond with ether-O atoms in the polymer chain. Furthermore, this study also indicates that the hand part is always more flexible than the core part, which improves the mobility of Li+. This study provides valuable insights into the dynamics of 4armPEO and highlights the role of LiTFSI in its performance. These findings have important implications for the development of advanced polymer electrolytes in energy storage applications.

Research at the BASIS of the ORNL's Spallation Neutron Source was sponsored by the Scientific User Facilities Division, Office of Basic Energy Sciences, U.S. Department of Energy.

References

[1] J.W. Choi, D. Aurbach, Nat. Rev. Mater. **1**, 4 (2016).
[2] V. Etacheri, R. Marom, R. Elazari, G. Salitra, D. Aurbach, Energy Environ. Sci. **4**, 3243 (2011).
[3] O.W. Sheng, C.B. Jin, J.M. Luo, H.D. Yuan, H. Huang, Y.P. Gan, J. Zhang, Y. Xia, C. Liang, W.K. Zhang, X.Y. Tao, Nano Lett. **18**, 3104 (2018).
[4] X. Zhang, T. Liu, S.F. Zhang, X. Huang, B.Q. Xu, Y.H. Lin, B. Xu, L.L. Li, C.W. Nan, Y. Shen, J. Am. Chem. Soc. **139**, 13779 (2017).
[5] F. Croce, G.B. Appetecchi, L. Persi, B. Scrosati, Nature (London) **394**, 456 (1998).
[6] A. M. Stephan, K. S. Nahm, Polymer **47**, 5952 (2006).
[7] F. B. Dias, L. Plomp, J. B. J. Veldhuis, J. Power Sources **88**, 169 (2000).
[8] R. J. Chen, W. J. Qu, X. Guo, L. Li, F. Wu, Mater. Horizon. **3**, 487 (2016).
[9] C. Do, P. Lunkenheimer, D. Diddens, M. Götz, M. Weiß, A. Loidl, X. G. Sun, J. Allgaier, M. Ohl, Phys. Rev. Lett. **111**, 018301 (2013).
[10] J. Allgaier et al. unpublished data.
[11] H. Wang et al. unpublished data.
[12] E. Mamontov, K. W. Herwig, Rev. Sci. Instr., **82**, 85109 (2011).
[13] F. Volino and A. Dianoux, Mol. Phys., **41**, 271–279 (1980).
[14] A. J. O'Malley, M. Sarwar, J. Armstrong, C. R. A. Catlow, I. P. Silverwood, A. P. E. York and I. Hitchcock, Phys. Chem. Chem. Phys., **20**, 11976-11986 (2018).
[15] V. G. Sakai, J. K. Maranas, I. Peral, J. R. D. Copley, Macromolecules, **41**, 10 (2008).